Final Draft
of the original manuscript:

Fischer-Bruns, I.; Feichter, J.; Kloster, S.; Schneidereit, A.:
How present aerosol pollution from North America impacts North Atlantic climate
In: Tellus A (2010) Blackwell Munksgaard

DOI: /10.1111/j.1600-0870.2010.00446.x

How present aerosol pollution from North America impacts North Atlantic climate

I. FISCHER-BRUNS[1]*, J. FEICHTER[2], S. KLOSTER[3], and A. SCHNEIDEREIT[4]

[1]*Max-Planck-Institut für Meteorologie, Hamburg, Germany. Now at: Climate Service Center–Germany, GKSS Forschungszentrum Geesthacht, Hamburg, Germany;* [2]*Max-Planck-Institut für Meteorologie, Hamburg, Germany;* [3]*Department of Earth and Atmospheric Sciences, Cornell University, Ithaca, NY, USA. Now at: Max-Planck-Institut für Meteorologie, Hamburg, Germany;* [4]*Meteorologisches Institut, Universität Hamburg, Germany*

Abstract

This paper describes the potential effects of present day aerosol pollution from North America (USA, Canada) on the climate of the North Atlantic region. The study has been performed by applying the comprehensive atmospheric general circulation model ECHAM5-HAM, which is coupled to a mixed-layer ocean with an embedded thermodynamic sea ice module. The model includes a microphysical aerosol model (HAM), which allows for the assessment of aerosol impacts on climate. Sulfate, black and organic carbon, sea salt and mineral dust are considered as aerosol species. Two equilibrium simulations with two different aerosol pollutant scenarios are compared for each season. We investigate the effect on radiation, temperature, hydrological quantities and dynamics, when human-induced aerosol emissions from North America were omitted. The decrease of both direct and indirect aerosol effects induces a positive change in TOA (top of the atmosphere) radiative fluxes resulting in an overall warming in the whole region. Our results demonstrate the vulnerability especially of the Arctic to the reduction in aerosol load. For fall we find an increase in precipitation over the North Atlantic, associated with a tendency to a larger number of cyclones with high pressure gradients and a higher frequency in storm days.

*Corresponding author.
e-mail: irene.fischer-bruns@gkss.de

1 Introduction

Climate models indicate globally increasing temperatures due to the anthropogenically induced greenhouse warming. However, the emission of heat-trapping gases like carbon dioxide is not the only climate-forcing factor caused by human activities. Aerosol particles are thought to contribute to climate change as well. They scatter and absorb solar radiation, hence affecting the radiative transfer through the atmosphere. Moreover aerosols act as cloud condensation nuclei (CCN) and thus influence cloud microphysics.

Aerosols like sea-salt particles, mineral dust, sulfate and organic carbon mainly scatter radiation, which causes a cooling of the Earth's surface. Black carbon, however, absorbs radiation and has thus a warming effect on climate. In particular, the sulfate and black carbon aerosol cycles, which appear to have a pronounced climate effect (Haywood and Boucher, 2000; Liepert et al., 2004; Lohmann and Feichter 2005), are strongly perturbed by anthropogenic emissions. Emissions of carbonaceous and sulfate aerosols originate particularly from combustion of coal, oil, and biomass. The aerosol population evolved consists of a spatially inhomogeneous and complex mixture of sulfates, organic carbon and black carbon, which can both absorb and reflect incoming sunlight, thus exerting both cooling the surface and warming the atmospheric layers. Whether the aerosols exert an overall warming or a cooling effect depends not only on the chemical composition and the size distribution of the particles, but also on the albedo of the underlying surface. Thus, a quantification of the aerosol's contribution to climate change is highly complex (e.g. Stier et al., 2007). In addition, aerosol cycles depend on the climate state, as aerosol and water cycles are tightly coupled (Feichter et al., 2004). Thus, quantification of the impact of aerosols on climate is hampered by several uncertainties. Aerosols influence not only climate but cause also a variety of adverse health impacts (WHO, 2003). Therefore, aerosol emissions are largely policy regulated so that many regions that have encountered large increases in aerosol emissions in the past, have reversed this trend towards decreasing aerosol emissions (Cofala et al., 2007).

Transport and removal of aerosols as well as chemical transformation processes are controlled by regional weather conditions and –from a long-term perspective– by the mean seasonal climate conditions. In this model study we investigate the role of anthropogenic aerosol pollution (due to emissions from energy production, industries, traffic and households) in North America on the North Atlantic climate. The climate of the North Atlantic is known to exhibit a considerable naturally driven variability over a wide range of time scales. Aerosols that are transported by the mid-latitude westerly winds from North America across the Atlantic Ocean may have impacts on local weather systems and the climate state in the Atlantic-European region, and vice versa.

We are especially interested in possible changes in TOA (top of the atmosphere) radiative fluxes and temperature distribution resulting probably in a modified atmospheric circulation due to anthropogenically produced aerosol pollution emitted from the North American continent. For that purpose we compare two equilibrium simulations performed with the global general circulation model ECHAM5 (Roeckner et al., 2003) extended by the microphysical aerosol model HAM (Stier et al., 2005). In a reference simulation all present-day aerosol emissions are considered. The second simulation assumes the hypothetical case that all anthropogenic aerosol and aerosol precursor emissions originating in North America are zero. Volcanic emissions are excluded as well. The study mainly aims at comparing the different scenarios. We describe the model and our methods in Section 2, and present the results in Section 3. The work is summarized and concluded in Section 4.

2 Methods

2.1 Climate model

The simulations reported here were conducted with the global atmospheric general circulation model ECHAM5 developed at the Max Planck Institute for Meteorology, Germany (Roeckner et al., 2003). The atmospheric model is extended by a complex microphysical aerosol model HAM (Stier et al., 2005). The atmospheric horizontal resolution is T63 in spectral space which corresponds to about 1.8°×1.8° on a Gaussian grid. The vertical resolution of 31 levels extends from the surface up to 10 hPa. ECHAM5-HAM is coupled to a mixed-layer ocean including a thermodynamic sea-ice module (Roeckner et al., 1995). In this simplified ocean model the oceanic heat transport is pre-calculated as monthly mean values in order to generate present-day sea surface temperatures as observed, whereas the sea surface temperatures and the sea ice are responding to the applied forcings.

In the microphysical aerosol model HAM, the following major aerosol compounds in the atmosphere are considered: sulfate (SO_4), black carbon (BC), organic carbon (OC), sea salt and mineral dust. HAM provides a prognostic treatment of the size-distribution, aerosol composition and mixing state of the different aerosol types for a superposition of seven log-normal modes (Vignati et al., 2004). It treats gas-phase and cloud liquid-phase sulfur chemistry, the nucleation of new sulfate particles and condensation of sulfate on pre-existing particles, coagulation, the transfer of particles from the insoluble to the soluble modes, and the thermodynamic equilibrium with the water vapor. Processes like wet and dry aerosol deposition and sedimentation are treated interactively dependent of the aerosol composition and size. An aerosol-cloud microphysical scheme is included in the HAM model, which accounts for the semi-direct and indirect aerosol effects on large-scale (stratiform) clouds (Lohmann et al., 2007). The different aerosol fields interact with the radiation processes considered in ECHAM5.

The emissions of sulfur dioxide (SO_2), BC, and OC are prescribed. Emissions of sea salt, mineral dust and DMS (Dimethylsulfide) from the marine biosphere are calculated interactively. In order to determine the formation of sulfate from DMS and SO_2 through oxidation processes, a sulfur chemistry scheme (Feichter et al., 1996) is applied which uses prescribed offline oxidant concentrations (Dentener et al., 2005; for more details see also Kloster et al., 2008).

A full evaluation of model performance is beyond the scope of this study. ECHAM5-HAM has been evaluated in detail with respect to aerosol and aerosol-cloud physics (Stier et al., 2004, Lohmann et al., 2007). Our study applied an identical emission inventory (Cofala et al., 2007) as described in Kloster et al. (2008). For an evaluation of the model, Kloster et al. (2008) have compared the simulated aerosol surface concentrations for SO_4, BC and POM (Particulate Organic Matter) with observations from the EMEP (http://www.emep.int) and the IMPROVE network (http://vista.cira.colostate.edu/improve/) for the year 2000. They overall found a good agreement, but an underestimation of simulated BC and POM surface concentrations over North America, which they relate to uncertainties in the emission inventory. As a consequence, the climate response to the omission of aerosol emissions from North America is likely to be on the lower side in the current study.

2.2 Simulation set up

We use ECHAM5-HAM for two equilibrium climate simulations with two different aerosol pollutant scenarios. Aerosol emissions, aerosol precursor emissions and GHG concentrations fixed at ‘year 2000’ values are prescribed in both simulations and kept constant during the whole model run. We use several decades to derive seasonal statistics of the model climate. Using

equilibrium simulations is statistically the most robust method to investigate the response of the climate system, since they capture the climate variations on annual and decadal timescales.

Our reference simulation (which has been performed earlier by Kloster et al., 2009) has been run over 100 yr (referred to as CTRL in the following). For the anthropogenic emissions of SO_2, BC and OC a recently designed aerosol emission inventory provided by IIASA (International Institute for Applied System Analysis) has been adopted (Cofala et al., 2007). For this study, seasonal means over the last 30 yr of CTRL have been analyzed. For comparison with CTRL we have performed an additional equilibrium simulation (referred to as EXP). In contrast to CTRL, in simulation EXP the anthropogenic aerosol emissions originating from combustion of fossil fuel (i.e. from energy production and industries, traffic and households) in North America (USA and Canada) are set to zero. Different from CTRL, here global volcanic sulfur emissions are excluded as well. The consideration of background volcanic sulfur emissions in CTRL contributes only a small uniform shortwave direct radiative forcing in our region of interest (cf. Graf et al. (1997), their Figure 6b). Compared to the impact of anthropogenic aerosols from North America, the contribution of volcanoes over the region investigated in this study is not important. The simulation EXP has been set up on the CTRL simulation, with the starting year chosen arbitrarily, and has been run for 50 yr. After 20 yr an equilibrium state was reached. We analyze seasonal means over the last 30 yr of this simulation.

According to this simulation set up, the reference simulation CTRL is representing the 'present-day' climate, and simulation EXP with suppressed man-made aerosols from North America represents the 'perturbed' case. Our analysis is based on the differences (EXP-CTRL) between the seasonal means[1] of both simulations. The interactively calculated natural emissions (DMS, sea salt, dust) differ only slightly between CTRL and EXP and are not further discussed. The significance of the differences between both 30-yr means is tested by the application of a Student's t-test at the 95% level.

2.3 Determination of storm frequency and cyclone tracking method

In Section 3.4 we analyze results obtained by an assessment of cyclone counts based on surface pressure (see this section, next paragraph) and the frequency of 'storm days', determined on the basis of maximum 10m wind speed data (Fischer-Bruns et al., 2005). This measure of storm frequency serves as a proxy for wind regimes and, in a broader sense, also for cyclonic activity. With this approach we avoid assumptions that have to be made when devising cyclone tracking algorithms, as described below for the method used here. The simulated maximum wind speed data are accessible in a high temporal resolution. They are determined by the model every 30 minutes and compared internally with the preceding value. The respective maximum over 6 hours is finally available as model output. We then determine the maximum value for each day at every grid point. As a threshold for 'storms' we use per definition the lower limit of the WMO (World Meteorological Organization) Beaufort wind speed scale of 8 Bft (17.2 ms^{-1}). In our notation a 'storm day' is counted if the daily near-surface maximum wind speed reaches or exceeds this threshold. The total mean number of storm days is determined for each season.

Cyclones are detected and tracked by an approved cyclone-identification algorithm developed by Blender et al. (1997). The method is based on the detection of a local minimum in the sea level pressure field or geopotential height field. For this study mean sea level pressure is chosen. The following assumptions have to be made: To avoid spurious detection, only minima persisting at least two days are detected. Furthermore the mean pressure gradient has to exceed at least 6 hPa/1000 km (corresponding roughly to a mean horizontal geopotential height gradient of 50 gpm/1000 km). Cyclone densities are obtained by determining the occurrences of pressure lows,

[1] The notation is: MAM for Northern Hemisphere spring, JJA for summer, SON for fall, and DJF for winter.

which are counted at each time step (6 hours as well), even if they remain at the same grid point. The cyclone density describes the number of pressure minima detections normalized by the number of time steps and the latitude dependent area associated with the resolution (here T63). The result is given in units per 1000^2 km^2 (~ 5°-latitude circle) multiplied by 100, and describes the occupation of this area by one ore more cyclones in % (e.g. a cyclone density of $100/1000^2$ km^2 would denote the permanent occupation of this area by one cyclone during the whole simulation period). For more details we refer to Sickmöller et al. (2000).

3 Results

The difference in aerosol and aerosol precursor emissions between EXP and CTRL are discussed in the following section. Here we show (Figure 1) annual means for CTRL on the global scale and the region with non-zero emission differences (EXP-CTRL), which is North America, according to our simulation set-up described in Section 2.2. In all further discussion (Figs. 2-6) we focus on seasonal (MAM, JJA, SON, DJF) changes in the North American/North Atlantic/European region (180°W–60E°, 0°–90°N). Figure 7 displays histograms related to characteristics of North Atlantic cyclones for autumn and winter (SON, DJF).

3.1 Emissions and Aerosol Optical Depth

The experimental set up is demonstrated in Figure 1. It shows annual means of the anthropogenic emissions of SO_2, BC and OC as prescribed in the reference simulation CTRL on a global scale and the resulting differences between EXP and CTRL for North America (180°W-20°W). Due to the limited oxidant concentration for winter, the oxidation of SO_2 generally yields the largest amount of sulfate for summer (cf. Roelofs et al., 2006). Moreover, during summer, the SO_2 is distributed over a larger volume of air that also has higher oxidant availability making its transformation more rapid (Rasch et al., 2000). As a result, the differences between EXP and CTRL in sulfate burden are largest for summer (not shown), whereas the differences are smallest for winter. Since the amount of aerosol in the atmosphere can also be characterized by the aerosol optical depth (AOD), we show seasonal differences between both simulations in terms of this quantity (Figure 2, left column). AOD is defined as the integrated extinction coefficient over the entire height of the atmosphere and expresses the degree to which aerosols prevent the transmission of incident light, mainly by scattering. In simulation EXP, the AOD is generally smaller due to the smaller aerosol load compared to CTRL. In accordance with the aerosol burden, significant differences in AOD are largest for summer, especially over the source regions of anthropogenic SO_2 emissions. The aerosol absorption optical depth (AAOD), which is shown in addition, is a measure that accounts for the extinction by absorption only. Differences in AAOD are mostly due to differences in BC burden (Figure 2, right column). They are significantly negative for all seasons, predominantly over the industrial regions of America, and largest for summer.

3.2 Changes in Radiative Fluxes

The changes in the TOA radiative fluxes due to the reduced aerosol emissions in EXP are calculated as the difference between the perturbed simulation EXP minus the reference simulation CTRL. We note that this method according to Kloster et al. (2008; 2009) is not in accordance with the standard IPCC definition of radiative forcing (Forster et al., 2007), which does not allow enabling feedback mechanisms. In our study, however, aerosol-cloud feedbacks are considered.

The resulting changes in clear-sky TOA radiative fluxes and all-sky TOA radiative fluxes between both simulations are determined by computing the differences (EXP-CTRL) in TOA net solar radiation under cloud-free and cloudy conditions (Figure 3, left and middle column). Positive differences in clear-sky net TOA radiative fluxes (left column) are due to less atmospheric backscattering of solar radiation on the one hand. On the other hand they are associated with less reflection due to surface albedo changes. Since the climate in EXP is warmer, a larger retreat of Arctic sea ice in comparison to CTRL occurs, associated with a reduction in albedo. This effect seems to dominate, since the largest positive differences in TOA radiative flux changes are found for spring and summer over the Arctic regions. They are reflecting the differences in ice margins between both simulations.

Additionally, changes in TOA radiative fluxes exist due to indirect effects, namely feedbacks resulting from the interaction between cloud and aerosol properties. Due to the pollution of the atmosphere by aerosols, the cloud properties can change. Since aerosol particles act as CCN, more droplets are formed and the average drop size decreases (under the assumption of fixed liquid water content, i.e. if feedback mechanisms are zero). Polluted clouds with more and smaller droplets are more reflective and have a larger lifetime, since it takes more time for small droplets to coalesce into droplets that are large enough to precipitate. The changes in all-sky TOA radiative fluxes (i.e. if cloud effects are considered) is positive in large regions over the Atlantic Ocean (Figure 3, middle column). This forcing is largest for summer due to most sunlight in this season, but possibly also due to a reduced cloud cover in EXP, as will be discussed in the following section.

Depending on the spatial non-uniformity and intermittency of the aerosol sources, the short atmospheric lifetime of the particles and microphysical and chemical interactions, the combined effects of the directly and indirectly induced changes in TOA radiative fluxes due to aerosols are generally characterized by large spatial and temporal heterogeneity. All these mechanisms obscure the detection of anthropogenic influence on the highly non-linear climate system. The temperature response and the response of hydrological variables to the reduced aerosol emissions are discussed in the following section as well.

3.3 Response of temperature and hydrological quantities

As has been shown in the last section, the overall net impact of the aerosols on the seasonal climate in the North Atlantic region is an enhancement of the backscattering of solar radiation associated with a surface cooling effect. According to our model set-up, and since we determine differences EXP-CTRL (and not vice versa), this effect is apparent by positive differences, i.e. by a warming. Figure 3 (right column) shows the geographical distribution of 2m temperature difference between both simulations. It is obvious that the Arctic region is the most vulnerable region especially for winter, when ice and snow cover is affected by the warming, as has been already addressed in the previous section.

In simulation EXP, fewer aerosols are emitted, resulting in less CCN. As a consequence, fewer clouds with less, but larger cloud droplets form. Thus, in EXP clouds have a shorter lifetime and a lower cloud albedo. This influences the radiation budget at the TOA and accounts for a warming effect as discussed before. Since the climate in EXP is warmer than in CTRL, more evaporation takes place, primarily from the oceans (Figure 4, left column). An increase in water vapor can, again, produce more warming through an enhanced greenhouse effect, and this warming can further enhance evaporation. However, it is not obvious that in a warmer climate and with larger evaporation cloud cover increases. Here, apparently due to changes in atmospheric circulation and stability, we find predominantly less cloud cover in EXP (Figure 4,

right column). This is in accordance with the results of most general circulation models, which generate fewer clouds in a warmer climate. Generally, the variability in cloud cover is large. In our study, significant differences in total cloud cover are small and can be found only over small areas for all seasons. Differences over the Atlantic Ocean are most obvious for fall.

As shown in Figure 5 (left column), for all seasons we find a significant reduction in vertically integrated cloud water, mainly over the Atlantic Ocean. This quantity is a measure for the precipitable water in the clouds. Largest differences occur for summer, where the difference in sulfate burden is largest (expressed in terms of AOD, Figure 2, left column). Yet, the differences in precipitation patterns are not significant over large areas of the North Atlantic Ocean (Figure 5, right column), at least for spring and summer. This is not surprising, since precipitation is also characterized by a large variability. Predominantly positive differences, probably due to the suppression of precipitation in CTRL as a consequence of a higher aerosol concentration compared to EXP, are significant only over the central North Atlantic for fall. Larger differences in precipitation patterns are also found in small bands near the equator due to a northward shift of the ITCZ (Intertropical Convergence Zone) in EXP. The reason for this shift is a higher temperature gradient between both hemispheres caused by the stronger warming of the Northern hemisphere in EXP (see also Kloster et al., 2009).

3.4 Dynamic response

Since baroclinic disturbances are most pronounced for fall and winter and in general these seasons exhibit the most intense extra-tropical storms, in this section we discuss results only for SON and DJF.

In order to estimate the occurrence of extreme wind speed events, we analyze the time series of maximum 10m wind speed at each grid point as described in section 2.3. In both simulations the largest frequency of storm days is found for winter in the well-known storm track region of the North Atlantic (not shown). Here the mean number of winter storm days is about up to 30 days in both simulations and exhibits no significant difference if compared with each other (Figure 6, left column). We find no significant differences for spring and summer as well, if aerosol emissions are reduced (not shown). This is the case only for fall. Here the average number of storm days amounts to maximum 30 in EXP but only up to 20 in CTRL (not shown), resulting in a significant positive difference of up to 10 storm days per season (Figure 6, left column, SON).

Due to the warming in EXP, we could expect that the response in cyclone density is similar to the response in simulations with increased GHG warming: in some model studies, a northward shift in cyclone density or storm frequency has been found for the Northern Hemisphere for winter (e.g. Bengtsson et al., 2006, Fischer-Bruns et al., 2005). However, in this study, the cyclone density difference patterns show significant values only in more or less spotted regions throughout all seasons. We find no significant shift in cyclone density, neither for fall nor for winter (Figure 6, right column). Instead, there is a slight tendency towards an increase in cyclone density near Iceland and a more clear decrease over the central North Atlantic for fall. For winter the pattern indicates that the cyclone tracks tend to have a more zonal component in EXP. However, there is no associated significant difference in the frequency of storm days as is found for fall.

Figure 7 shows related histograms of cyclone core pressure and mean pressure gradient for both simulations. Here only cyclones traveling over the North Atlantic region are considered. As can be seen from the histogram of the pressure gradient for SON (Figure 7, right column, upper graph), the number of depressions with large pressure gradients (more than 25 hPa/1000 km) is larger in EXP compared to CTRL. This is consistent with the increase of storm frequency for

SON (Figure 6, left column) and also in accordance with results obtained by e.g. Leckebusch and Ulbrich (2004) and Bengtsson et al. (2009), who, however, both investigate cyclone behavior in a GHG scenario. Leckebusch and Ulbrich (2004) find changes of extreme cyclone systems, especially a tendency towards more extreme wind events caused by deepening cyclones for several regions in Europe. Bengtsson et al. (2009) discover an increase of core pressures in extra-tropical cyclones. This is consistent with our results, since the occurrence of cyclones with core pressures smaller than 990 hPa is larger in EXP than in CTRL (Figure 7, left column). The histograms of cyclone core pressure and mean pressure gradient for winter generally match those for fall, although the distribution in core pressure seems to be a bit broader for winter. However, no significant differences in storm day frequency for winter can be detected, as has been discussed before.

4 Summary and Conclusions

Based on two equilibrium climate simulations we investigate the climate response to a hypothetical forcing, where anthropogenic aerosol emissions from North America are omitted. Our study is done using a coupled model system consisting of the atmospheric component ECHAM5 (T63), a thermodynamic sea ice model and a mixed-layer ocean. The atmospheric model includes the microphysical aerosol model HAM. Aerosol and water cycle as well as the atmospheric dynamics are coupled fully and interactively. Our main results of a simulation, where the anthropogenic emissions from North America are set to zero, are as follows:

1. The combined effects of the directly and indirectly induced changes in TOA radiative fluxes at the top of the atmosphere turn out to be predominantly positive corresponding to a warming effect. Our results demonstrate the vulnerability of the Arctic region to a warming as a consequence of the reduction in anthropogenic aerosols that are mostly scattering.
2. It is pointed out that cloud effects exhibit a different picture in TOA radiative flux changes – compared to the changes in radiative fluxes induced by the direct aerosol effect alone – towards stronger changes in radiative fluxes, especially over the Atlantic Ocean and for summer.
3. To some extent, we find less total cloud cover for all seasons. Over the central North Atlantic Ocean, predominantly positive mean seasonal differences in precipitation are significant for fall.
4. For fall, also a larger frequency in storm days is found, corresponding to a larger number of cyclones with higher pressure gradients developing over the central North Atlantic.

This study suggests that, although our results are restricted to the North Atlantic region, reductions in anthropogenic aerosol emissions can generally contribute to an increase in surface temperature and consequently to a modification of the water cycle components and the atmospheric dynamics. Vice versa, this implies that temperatures can decrease due to high aerosol concentrations. Thus the presence of aerosols has the potential to partially offset effects caused by temperature increases due to anthropogenic GHGs. Our findings are consistent with results from a recent study by Shindell and Faluvegi (2009), which emphasizes that compared to the tropics and the Southern Hemisphere, the extratropics of the Northern Hemisphere are much more sensitive to local forcings.

Our study is limited in the sense that we make use of a mixed-layer ocean model, including a thermodynamic sea-ice module, for reasons of computational costs. This simplification implies thermodynamic interactions between atmosphere and sea ice only. Though, it does not allow for an impact of aerosol-induced changes in atmospheric dynamics on sea ice. Moreover, although our atmospheric model is relatively complex compared to most of the climate models used in the

IPCC AR4 assessment (IPCC, 2007), we understand that uncertainties in this study are also strongly related to cloud radiation feedbacks. The reason is that our model -like most, if not all major coupled climate models- has an insufficient representation of clouds. Yet, we emphasize with this study that climate change simulations require a treatment of the interactions between aerosol and cloud physics, as well as chemistry.

Acknowledgements

This work was funded by the 'Sonderforschungsbereich' (SFB) 512 sponsored by the 'Deutsche Forschungsgemeinschaft' (DFG). We thank Richard Blender for providing the tracking method and Johannes Quaas for helpful suggestions. We appreciate very much the help of Elisabeth Viktor and Norbert Noreiks in adapting the figures.

References

Bengtsson L., Hodges K. I. and Roeckner E. 2006. Storm Tracks and Climate Change. *J. Clim.* **19**, 3518-3543.

Bengtsson L., Hodges K. I. and Keenlyside N. 2009. Will extratropical Storms Intensify in a Warmer Climate? *J. Clim*. **22**, 2276-2301.

Blender R., Fraedrich K. and Lunkeit F. 1997. Identification of cyclone-track regimes in the North Atlantic. *Q.J.R. Meteorol. Soc.* **123**, 727-741.

Cofala J., Amann M., Klimont Z., Kupiainen K. and Höglund-Isaksson, L. 2007. Scenarios of global anthropogenic emissions of air pollutants and methane until 2030. *Atmos. Environ.* **41(38)**, 8486-8499.

Dentener F., Stevenson D., Cofala J., Mechler R., Amann M., Bergamaschi P., Raes F., Derwent R. 2005. The impact of air pollutant and methane emissions controls on tropospheric ozone and radiative forcing: CTM calculations for the period 1990-2030. *Atmos. Chem. Phys.* **5**, 1731-1755.

Feichter J., Kjellström E., Rodhe H., Dentener F., Lelieveld J., Roelofs G.J. 1996. Simulation of the tropospheric sulfur cycle in a global climate model. *Atmos. Environ.* **30 (10-11)**, 1693–1707

Feichter J., Roeckner E., Lohmann U. and Liepert B. 2004. Nonlinear Aspects of the Climate Response to Greenhouse Gas and Aerosol Forcing. *J. Clim.* **17**, 2384-2398.

Fischer-Bruns I., von Storch H., Gonzales-Rouco J.F. and Zorita E. 2005. Modelling the variability of midlatitude storm activity on decadal to century time scales. *Clim. Dyn.*, **25 (5)**, 461-476, doi:10.1007/s00382-005-0036-1.

Forster P., Ramaswamy V., Artaxo P., Berntsen T., Betts R., Fahey D. W., Haywood J., Lean J., Lowe D. C., Myhre G., Nganga J., Prinn R., Raga G., Schulz M. and van Dorland R. 2007. Changes in Atmospheric Constituents and in Radiative Forcing. In: Climate Change 2007: The Physical Science Basis. Contribution of Working Group I to the Fourth Assessment Report of the Intergovernmental Panel on Climate Change [Solomon, S, Qin D, Manning M, Chen Z, Marquis M, Averyt KB, Tignor M and Miller HL (eds.)]. Cambridge University Press, Cambridge, United Kingdom and New York, NY, USA.

Graf H.-F., Feichter J. and Langmann B. 1997. Volcanic degassing: Contribution to global sulphate burden and climate. *Journ. Geophys. Res.* **102**, 10727-10738.

Haywood J. and Boucher O. 2000. Estimates of the direct and indirect radiative forcing due to tropospheric aerosols: A review. *Rev. Geophys.* **38 (4)**, 513-543

Horowitz, L. W., Walters, S., Mauzerall, D. L., Emmons, L. K., Rasch, P. J., Granier, C., Tie, X. X., Lamarque, J. F., Schultz, M. G., Tyndall, G. S., Orlando, J. J., and Brasseur, G. P. 2003. A global simulation of tropospheric ozone and related tracers: Description and evaluation of MOZART, version 2.J. *Geophys. Res.* **108 (D24)**, 4784, doi:10.1029/2002JD002853.

IPCC. 2007. 'Climate Change 2007: The Physical Science Basis' written by Working Group I to the Fourth Assessment Report of the Intergovernmental Panel on Climate Change (IPCC).

Kloster S., Dentener F., Feichter J., Raes F., van Aardenne J., Roeckner E., Lohmann U., Stier P. And Swart R. 2008. Influence of future air pollution mitigation strategies on total aerosol radiative forcing. *Atmos. Chem. Phys.* **8**, 6405-6437.

Kloster S., Dentener F., Feichter J., Raes F., Lohmann U., Roeckner E. and Fischer-Bruns I. 2009. A GCM study of future climate response to aerosol pollution reductions. *Clim. Dyn*. doi: 10.1007/ s00382-009-0573-0.

Leckebusch, G.C. and Ulbrich U. 2004. On the relationship between cyclones and extreme windstorm events over Europe under climate change. *Global Planet. Chang*e **44**, 181-193.

Liepert B., Feichter J., Lohmann U. and Roeckner E. 2004. Can aerosols spin down the water cycle in a warmer and moisture world? *Geophys. Res. Lett.* **31 (L06207)**, doi:10.1029/2003GL019060.

Lohmann U. and Feichter J. 2005. Global indirect aerosol effects: A review. *Atmos. Chem. Phys.* **5**, 715-737.

Lohmann U., Stier P., Hoose C., Ferrachat S., Roeckner E. and Zhang J. 2007. Cloud microphysics and aerosol indirect effects in the global climate model ECHAM5-HAM. *Atmos. Chem. Phys.* **7**, 3425-3446.

Rasch P. J., Barth M. C. and Kiehl J. T. 2000. A description of the global sulphur cycle and its controlling processes in the National Center for Atmospheric Research Community Climate Model, Version 3. *Journ. Geophys, Res.* **105 (D1)**, 1367-1385.

Roeckner E., Siebert T. and Feichter J. 1995. Climatic response to anthropogenic sulfate forcing simulated with a general circulation model. Aerosol Forcing of Climate, R. J. Charlson and J. Heintzenberg, Eds., John Wiley and Sons, 349–362.

Roeckner E., Baeuml G., Bonventura L., Brokopf R., Esch M., Giorgetta M., Hagemann S., Kirchner I., Kornblueh L., Manizini E., Rhodin A., Schlese U., Schulzweida U. and Tompkins A. 2003. The atmospheric general circulation model ECHAM5. Part I: Model description, report 349, Max Planck Institute for Meteorology, Hamburg, Germany. Available from: http://www.mpimet.mpg.de.

Roelofs G. J., Stier P., Feichter J., Vignati E. and Wilson J. 2006n Aerosol activation and cloud processing in the global aerosol-climate model ECHAM5-HAM. *Atmos. Chem. Phys.* **6**, 2389-2399.

Shindell D. and Faluvegi G. 2009. Climate response to regional radiative forcing during the twentieth century. *Nature Geosci.* **2**, 294-300, doi: 10.1038/ngeo473.

Sickmöller M., Blender R. and Fraedrich K. 2000. Observed winter cyclone tracks in the northern hemisphere in re-analysed ECMWF data. *Q. J. R. Met. Soc*. **126** 591-620. doi: 10.1002/ qj.49712656311.

Stier P., Feichter J., Kinne S., Kloster S., Vignati E., Wilson J., Balkanski Y., Schulz M., Ganzeveld L., Werner M., Tegen I., Boucher O., Minikin A. and Petzold A. 2005. The aerosol-climate model ECHAM5-HAM. *Atmos. Chem. Phys.* **5**, 1125-1156.

Stier P, Feichter J., Kloster S., Vignati E., Wilson J. 2006. Emission-Induced Nonlinearities in the Global Aerosol System - Results From the ECHAM5-HAM Aerosol-Climate Model. *J. Clim.* **19 (16)**, 3845-3862.

Stier P., Seinfeld J. H., Kinne S. and Boucher O. 2007. Aerosol absorption and radiative forcing. *Atmos. Chem. Phys.* **7**, 5237-5261.

Vignati E., Wilson J. and Stier P. 2004. M7, An efficient size-resolved aerosol microphysics module for large-scale aerosol transport model. *Journ. Geophys Res.* **109 (D22202)**. doi: 10.1029/2003JD004485.

WHO. 2003. Health aspects of air pollution with particulate matter, ozone and nitrogen dioxide. Report on a WHO Working group, Bonn, Germany. Available at: http://www.euro.who.int/ document/e79097.pdf

Figures

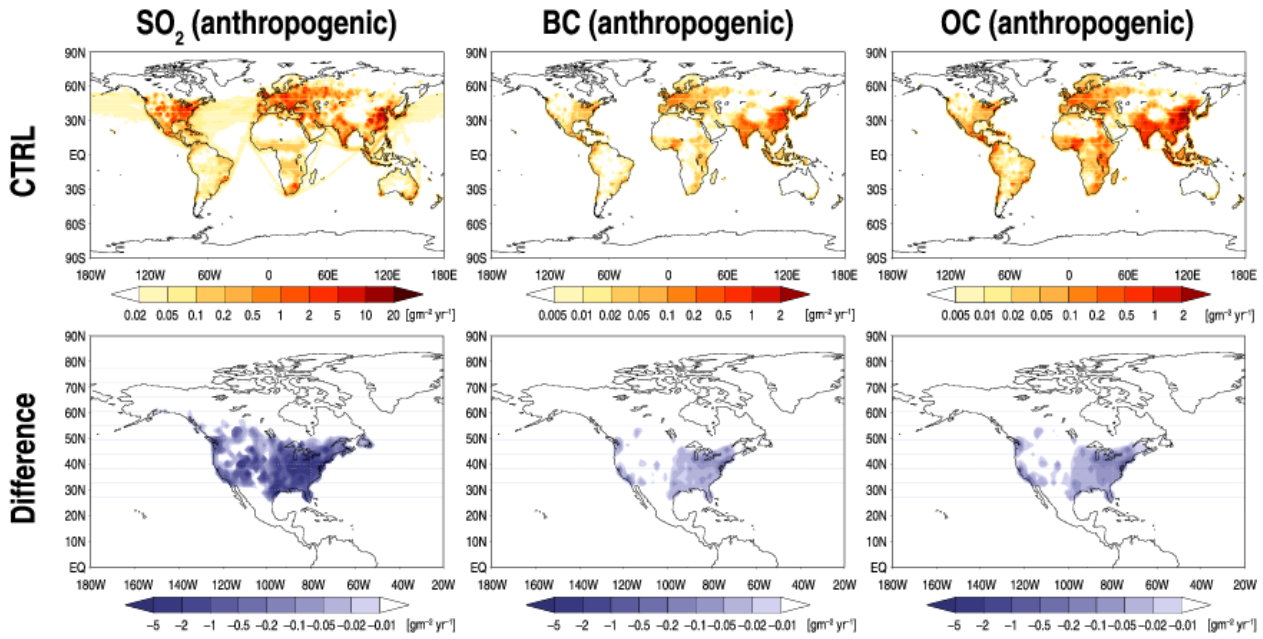

Figure 1 *Upper panels:* Global anthropogenic emissions of SO_2, BC and OC as prescribed in CTRL. *Lower panels:* Differences (EXP-CTRL) in emissions for the Northern hemispheric sector due to the omission of anthropogenic aerosol and aerosol precursor emissions from North America in simulation EXP. All panels show annual means [gm^{-2} yr^{-1}].

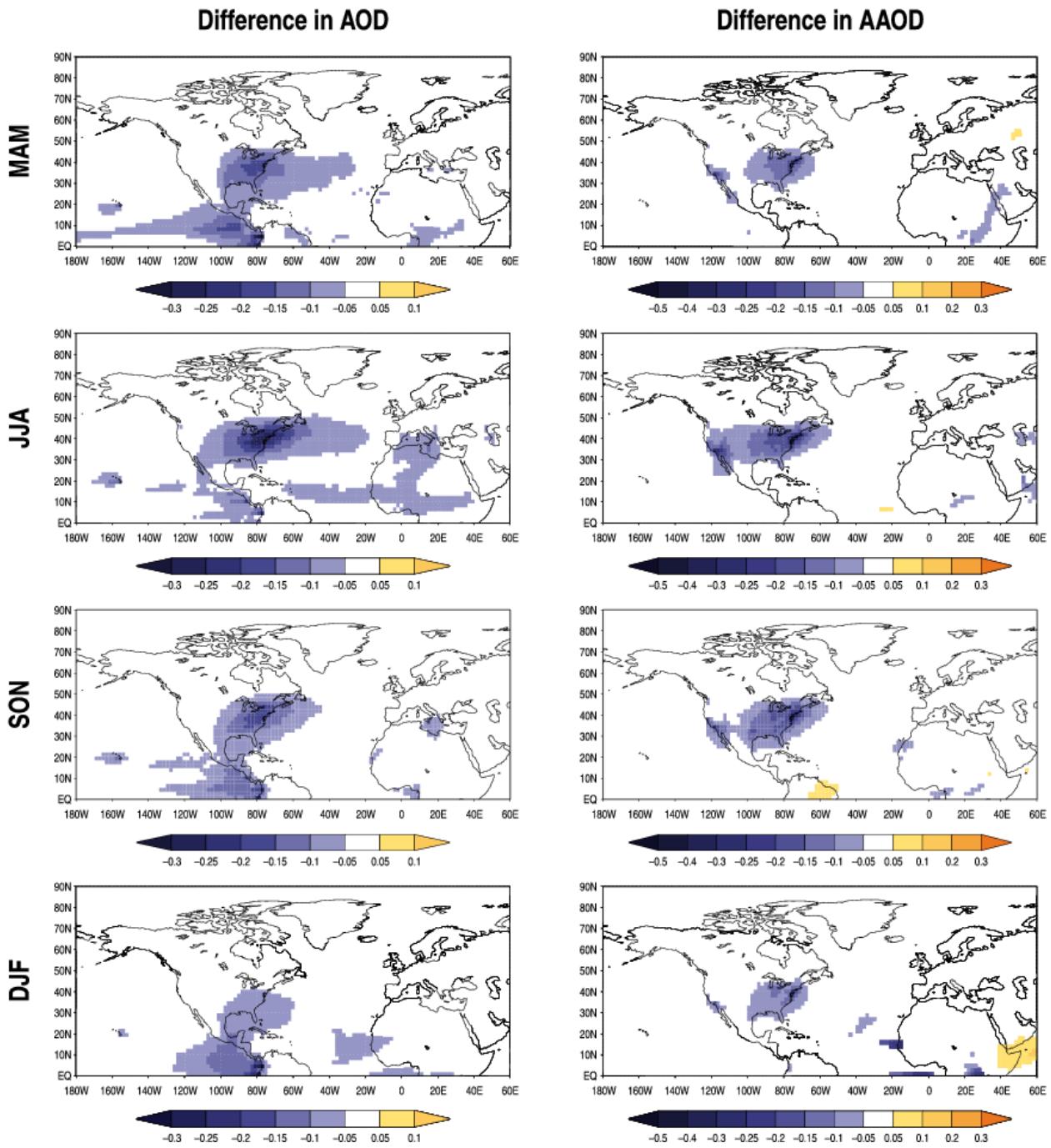

Figure 2 Seasonal differences (EXP-CTRL) between both simulations in aerosol optical depth (AOD), and aerosol absorption optical depth **(**AAOD), both referring to a mid-visible wavelength of λ=550 nm [dimensionless units]. Units for AAOD are multiplied by a factor of 100. Areas where the differences are not statistically significant at the 95% level are masked white.

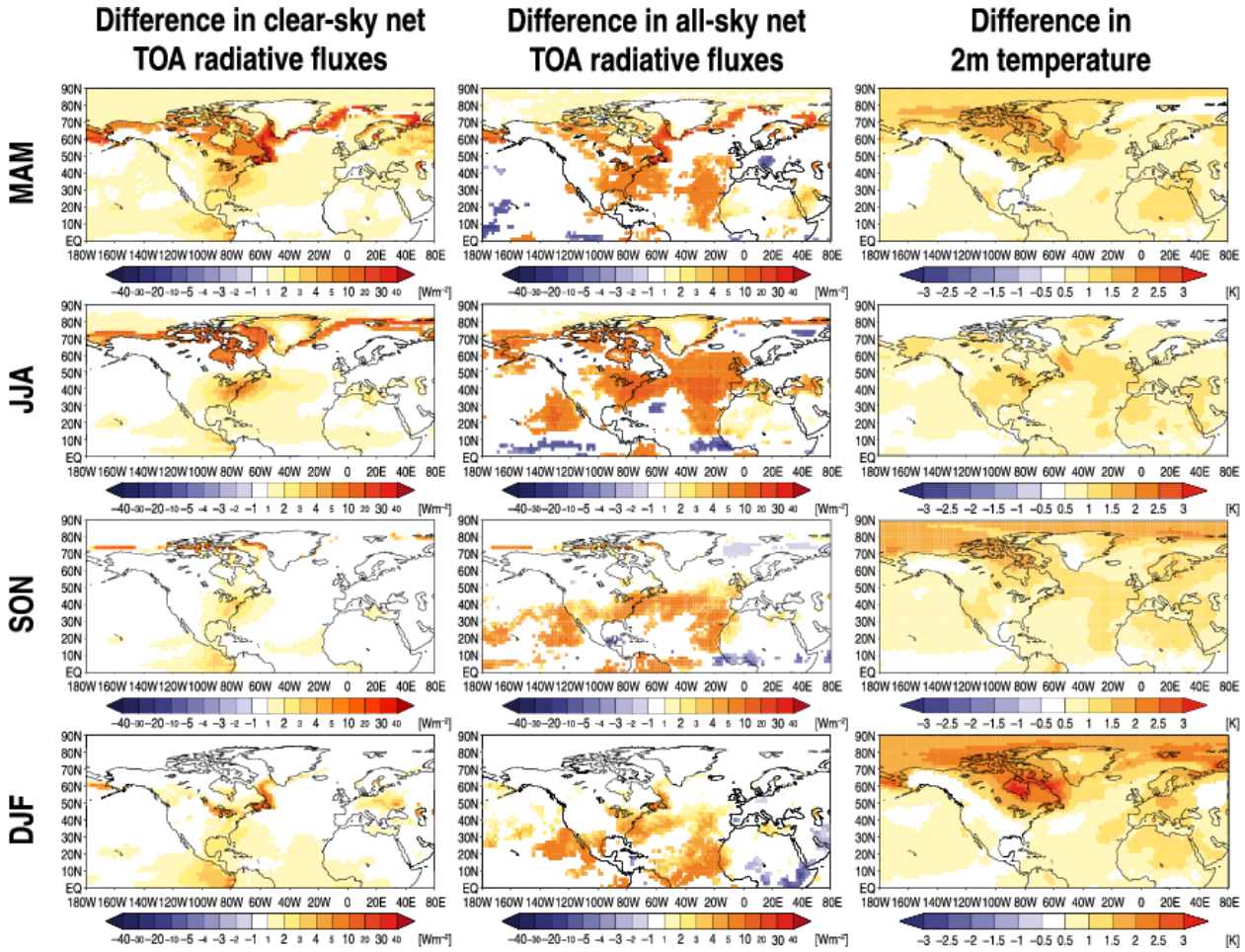

Figure 3 Seasonal differences (EXP-CTRL) between both simulations in clear-sky and in all-sky net TOA radiative fluxes [Wm^{-2}]. (The annual global difference (EXP-CTRL) in all-sky net TOA radiative fluxes is 1.17 Wm^{-2}). Right panel: Seasonal differences (EXP-CTRL) in 2m temperature [K]. Areas where the differences are not statistically significant at the 95% level are masked white.

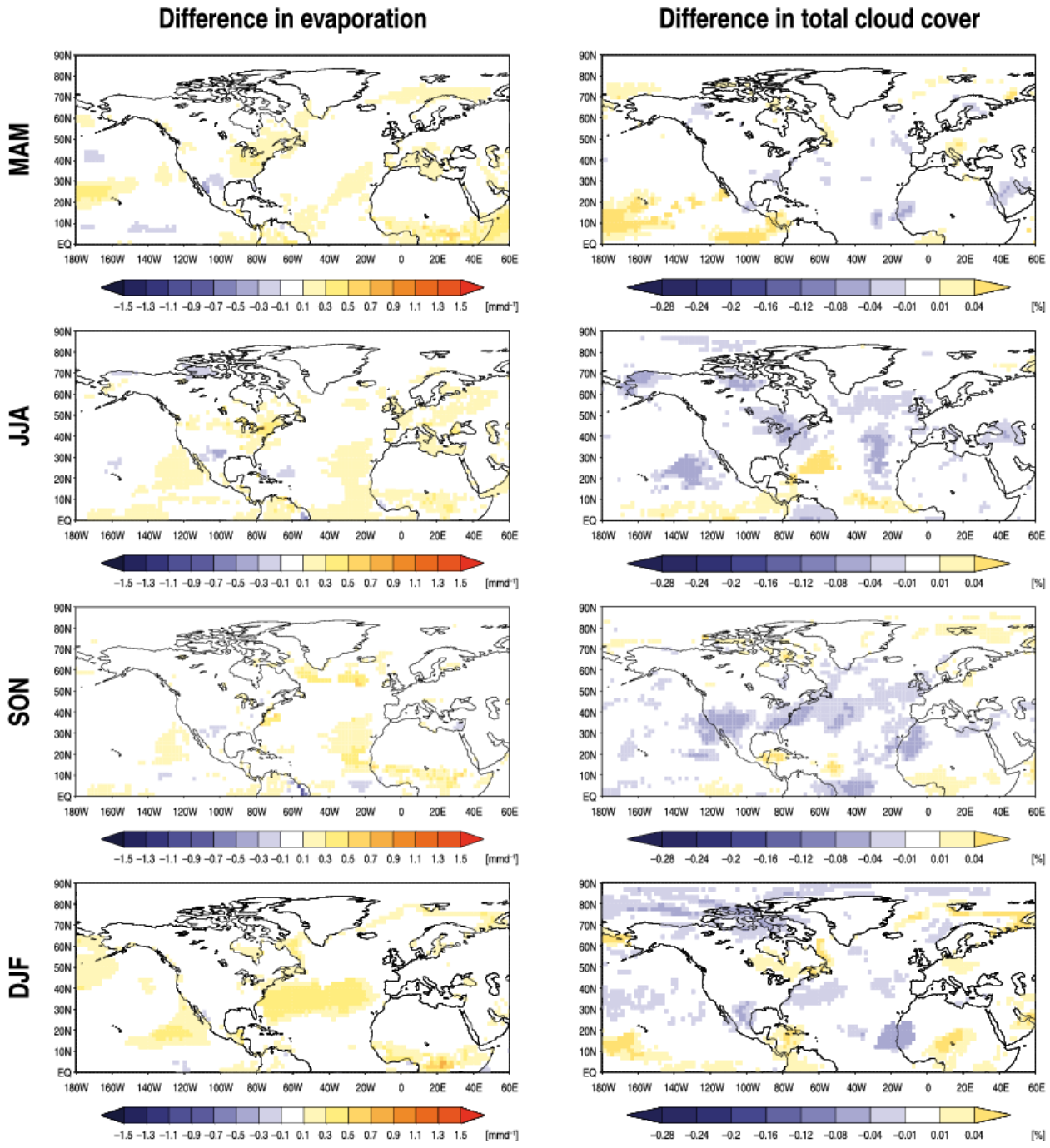

Figure 4 Seasonal differences (EXP-CTRL) between both simulations in evaporation [mmd^{-1}] and total cloud cover [%]. Areas where the differences are not statistically significant at the 95% level are masked white.

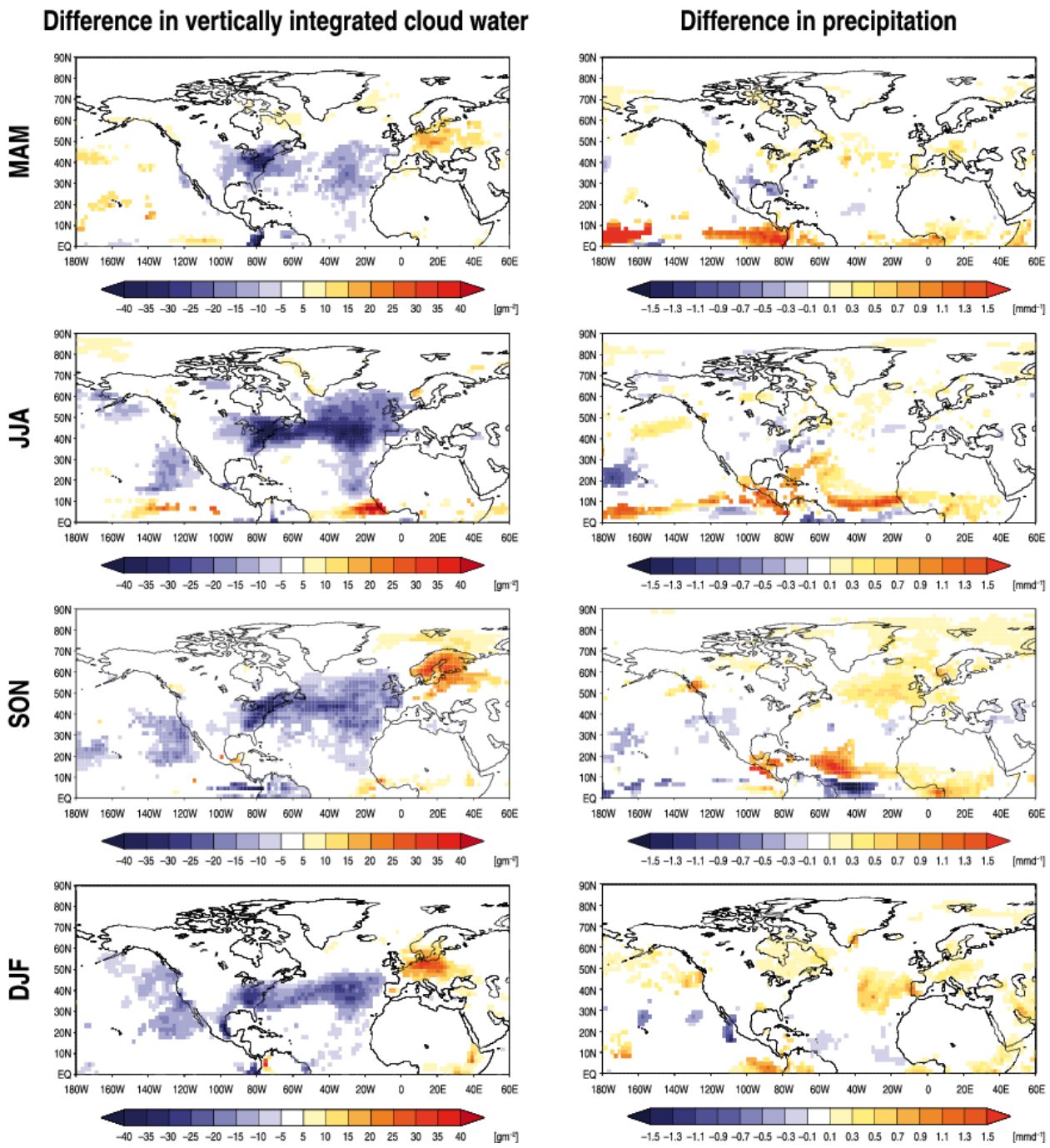

Figure 5 Seasonal differences (EXP-CTRL) between both simulations in vertically integrated cloud water [gm^{-2}] and precipitation [mmd^{-1}]. Areas where the differences are not statistically significant at the 95% level are masked white.

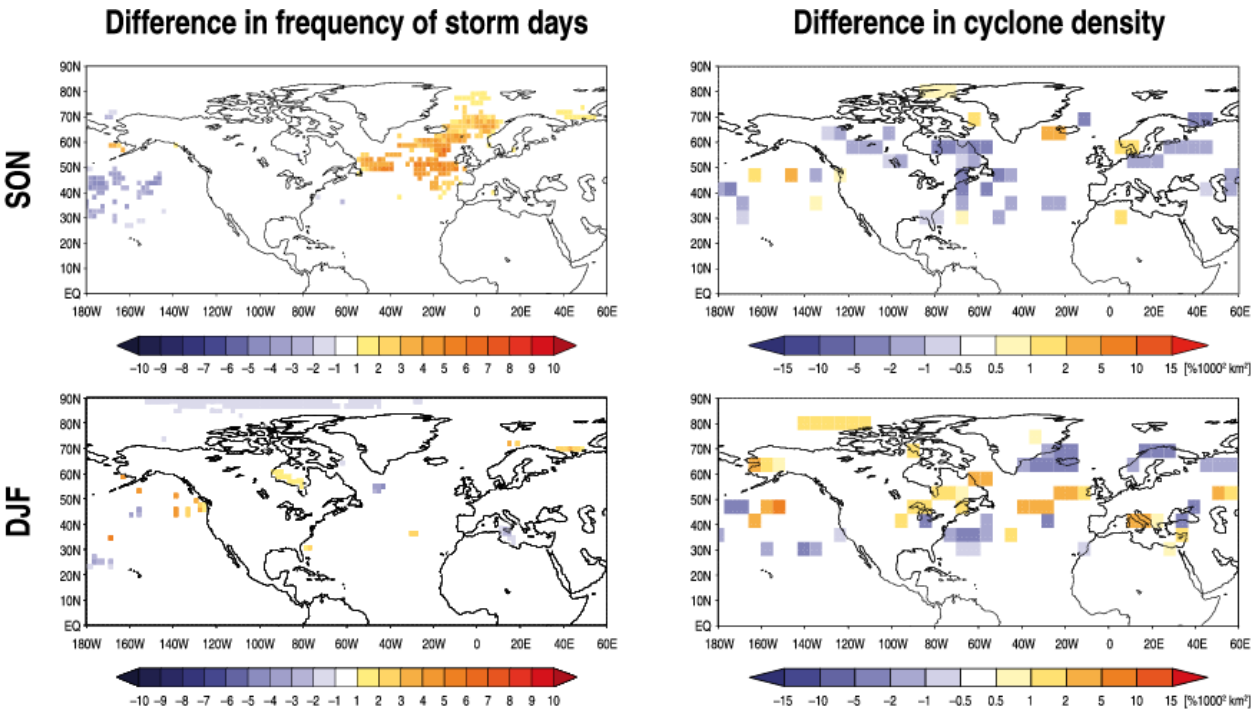

Figure 6 Seasonal differences (EXP-CTRL) between both simulations in frequency of storm days [dimensionless units] and cyclone density [%/1000^2 km^2] for autumn and winter. Cyclone densities are analyzed only for latitudes between 20°–90°N. Areas where the differences are not statistically significant at the 95% level are masked white.

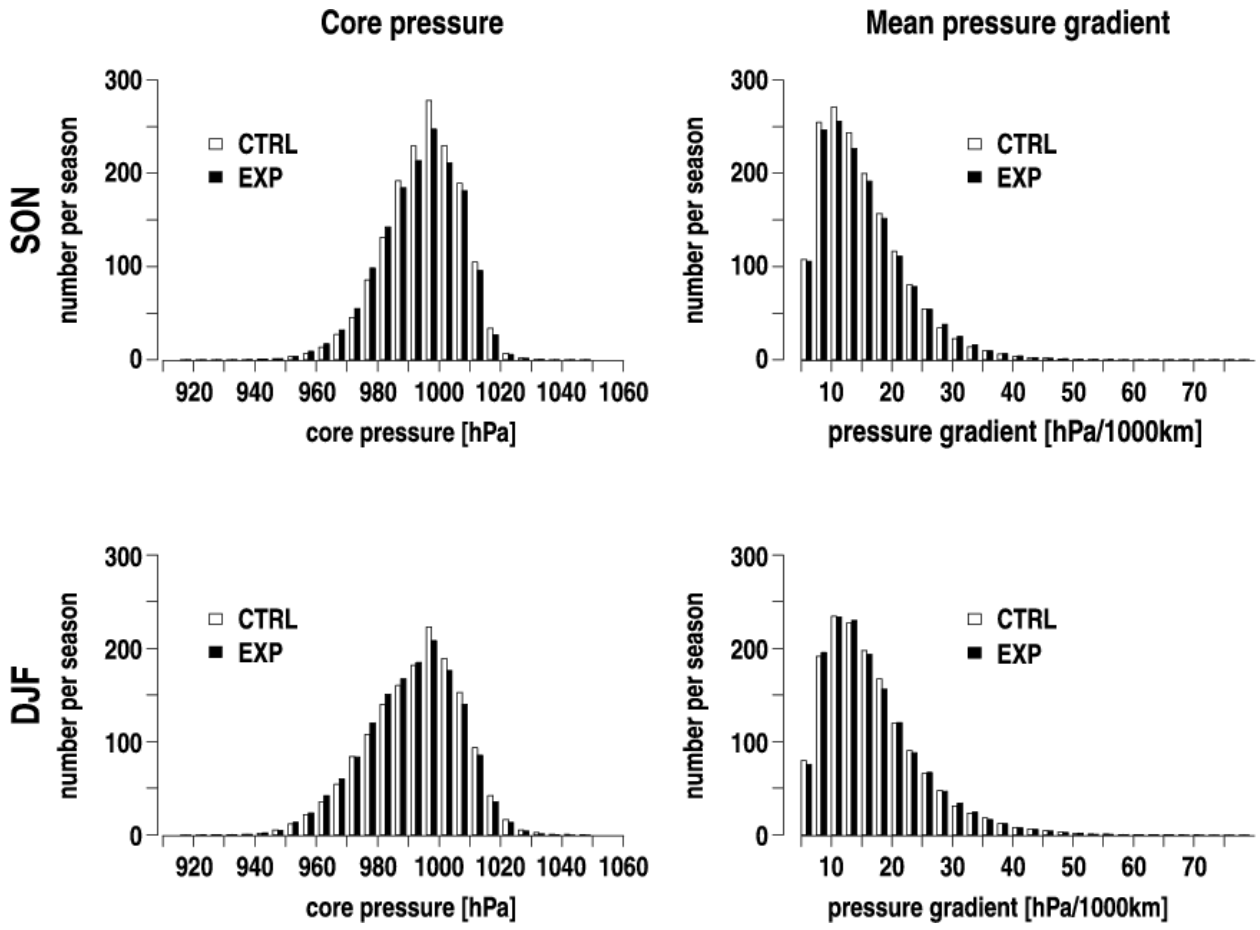

Figure 7 Histograms of North Atlantic cyclone core pressure [hPa] and mean pressure gradient [hPa /1000 km] for fall and winter.